NUCL SCI TECH (2019) 30:26
https://doi.org/10.1007/s41365-019-0547-9

Enhanced removal of X-ray-induced carbon contamination using radio-frequency Ar/H_2 plasma

Yi Wang[1,2] · Qi-Peng Lu[1] · Yun-Guo Gao[1] · Xue-Peng Gong[1] · Yuan Song[1]

Received: 13 December 2017 / Revised: 21 June 2018 / Accepted: 6 August 2018 / Published online: 18 January 2019

Abstract Removal of X-ray-induced carbon contamination on beamline optics was studied using radio-frequency plasma with an argon/hydrogen (Ar/H_2) mixture. Experiments demonstrated that the carbon removal rate with Ar/H_2 plasma was higher than that with pure hydrogen or argon. The possible mechanism for this enhanced removal was discussed. The key working parameters for Ar/H_2 plasma removal were determined, including the optimal vacuum pressure, gas mixing ratio, and source power. The optimal process was performed on a carbon-coated multilayer, and the reflectivity was recovered.

Keywords Radio-frequency plasma · X-ray irradiation · Carbon contamination

1 Introduction

Under X-ray irradiation, residual hydrocarbons in a light source beamline will split into dissociated carbon atoms, which will deposit on the surface of optics to form contamination [1, 2]. This deposited carbon will result in a severe degradation of the reflectivity. X-ray sources have been developed to provide high energy, high power, and a strong pulse for third-generation synchrotron radiation sources [3, 4] and X-ray free-electron laser (XFEL) facilities [5]. The improvement in the source has in turn brought a serious challenge to the life of the X-ray optics due to carbon contamination. In order to extend the life of the X-ray optics, high efficiency carbon contamination removal methods should be implemented. This study is devoted to investigating the feasibility of high efficiency carbon removal with low-pressure plasma.

Practically, it is necessary to remove the carbon with reasonable efficiency, while the multilayer optics should not be harmed. Atomic hydrogen has been employed to solve the carbon removal problem [6, 7], but the removal rate of carbon contamination with atomic hydrogen is quite low, limiting its practical use. Therefore, radio-frequency (RF) plasma carbon removal technology has been widely studied [8–11]. Pellegrin et al. [8] investigated hydrogen and oxygen plasma removal of carbon-deposited specimens and determined that the removal efficiency with oxygen plasma was much higher than that with hydrogen plasma. However, there is also a risk of oxidation of the optics material and deterioration of the optical characteristics. Alternatively, the hydrogen plasma removal method could become the preferred one if its removal efficiency can be enhanced. The addition of argon to the RF hydrogen plasma is a promising way to improve the removal rate

This work was supported by the National Nature Science Foundation of China (No. 61404139), the National Science and Technology Major Project (No. 2012ZX0270 2001-005), and the State Key Laboratory of Applied Optics.

✉ Qi-Peng Lu
luqp@ciomp.ac.cn

✉ Yun-Guo Gao
gaoyg@ciomp.ac.cn

[1] State Key Laboratory of Applied Optics, Changchun Institute of Optics and Fine Mechanics and Physics, Chinese Academy of Sciences, Changchun 130033, China

[2] University of Chinese Academy of Sciences, Beijing 100039, China

[8, 11]. The mechanism of this enhancement was speculated in Ref. [8], which proposed that argon improves the transport of hydrogen, while Pradhan et al. [12, 13] argued that the enhancement was the result of kinetic effects.

In this study, carbon removal experiments using pure hydrogen, pure argon, and Ar/H_2 plasma were conducted separately to compare the removal rates with different methods. The optimal parameters for enhanced removal conditions with Ar/H_2 plasma were determined through a series of experiments. This optimal process was performed on a carbon-coated multilayer. Based on these experimental results, a possible removal mechanism has been proposed to explain the enhancement with Ar/H_2 plasma.

2 Experimental

In most cases, the type of deposited carbon induced by X-rays is amorphous. Therefore, magnetron-deposited carbon has frequently been used as a model for X-ray-induced carbon growth [3, 8, 14]. Thus, experiments were performed on a quartz wafer and multilayer optics coated with an amorphous carbon film with a thickness between 25 and 75 nm. The carbon film was deposited by a commercial magnetron sputtering source with a polycrystalline graphite target. For the specimens, the changes in the carbon thickness of the carbon-coated quartz wafers were monitored to demonstrate the removal efficiency. In addition, optimal parameters were determined using the quartz wafers. The change in reflectivity on the multilayer drives the study of the feasibility of carbon removal using an Ar/H_2 plasma.

As a plasma source, a commercially available RF plasma generator (Model GV10X "Downstream Asher", IBSS, San Francisco, CA, USA) was employed that utilized inductively coupled plasma (ICP). Relative to the specimens in the cleaning chamber, the plasma is generated in a separate volume upstream. The volume of the cleaning chamber is 28L, which is about 1000 times larger than that of the plasma chamber. A small orifice is located between the plasma chamber and the cleaning chamber, with a diameter of only 1 mm. The pressure in the cleaning chamber can be controlled with a gate valve, while the pressure in the discharge chamber can be adjusted with a throttle valve if necessary. This arrangement facilitates plasma generation at a higher pressure within the plasma operation pressure regime [15, 16], while a larger mean free path length of the reactant is produced in the cleaning chamber at lower pressure. The pressure gradient between these two chambers is helpful for the distribution of radical species across the cleaning chamber, which is compatible with the size of the optics. This "Downstream" style is shown in Fig. 1.

As shown in Fig. 2, the experimental apparatus includes a turbomolecular pump, backing pump, quartz crystal microbalance (QCM), vacuum gauge, plasma source, and residual gas analyzer (RGA). The high vacuum environment of the chamber is achieved through these pumps, and the mass flow controllers (MFC) not only control and display the gas flow of hydrogen and argon, but also adjust the ratio of the mixing gas. The RGA is used to detect the density of the residual gases in the chamber. The carbon removal rates and the change in carbon thickness are monitored by the QCM on the quartz wafers.

3 Results and discussion

3.1 Comparison of removal using Ar/H_2 and pure gas plasmas

Experiments with specimens were conducted to investigate carbon removal using an Ar/H_2 plasma. The removed thickness of carbon was monitored through the QCM. First, a pure hydrogen flow of 1 sccm was set by the MFC, and the plasma was ignited at a vacuum chamber pressure of 1×10^{-3} mbar by adjusting the gate valve (equivalent to changing the pumping speed of the turbomolecular pump). The surface of the carbon-coated quartz wafer was exposed to the hydrogen plasma, as shown in Fig. 3a. Next, the hydrogen flow of 1 sccm was preserved, while an argon flow of 2 sccm was introduced to ensure a gas ratio of 1:2. A vacuum chamber pressure of 1×10^{-3} mbar was maintained by adjusting the gate valve. The carbon-coated specimen was treated with the Ar/H_2 plasma, as shown in Fig. 3b. Finally, the carbon-coated specimen was treated with pure argon plasma at the same vacuum pressure, as shown in Fig. 3c.

The temperature sensor indicated that the temperature of the sample surface changed slightly during the above process and was slightly higher than room temperature. There was no difference in temperature among the three types of gas discharge plasma, as the plasmas were all under lower pressure. As mentioned above, the chamber pressure for all three types of gas discharge was adjusted close to 0.001 mbar by the gate valve. The power was supplied identically by the GV10X at 90 W. Therefore, the procedures shown in Fig. 3 were conducted under the same conditions (plasma generator, experimental apparatus, pressure, temperature, and power), and their differences lie only in the gas type and resulting plasma.

In Fig. 4, the changes in the carbon thickness have been shown only under stable conditions, and the non-steady testing results have been excluded. To compare the changes in the removal rates for the three steps in Fig. 3 more intuitively, both the initial carbon thickness and the start

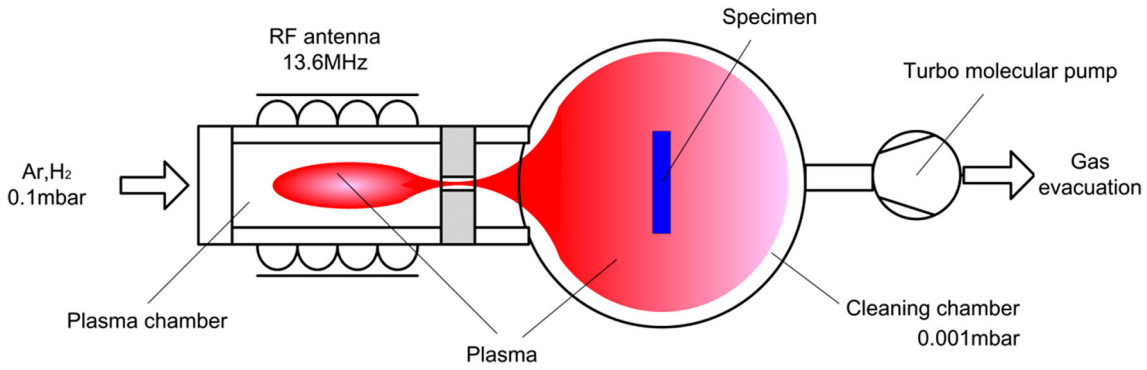

Fig. 1 (Color online) Schematic of the "Downstream" work style

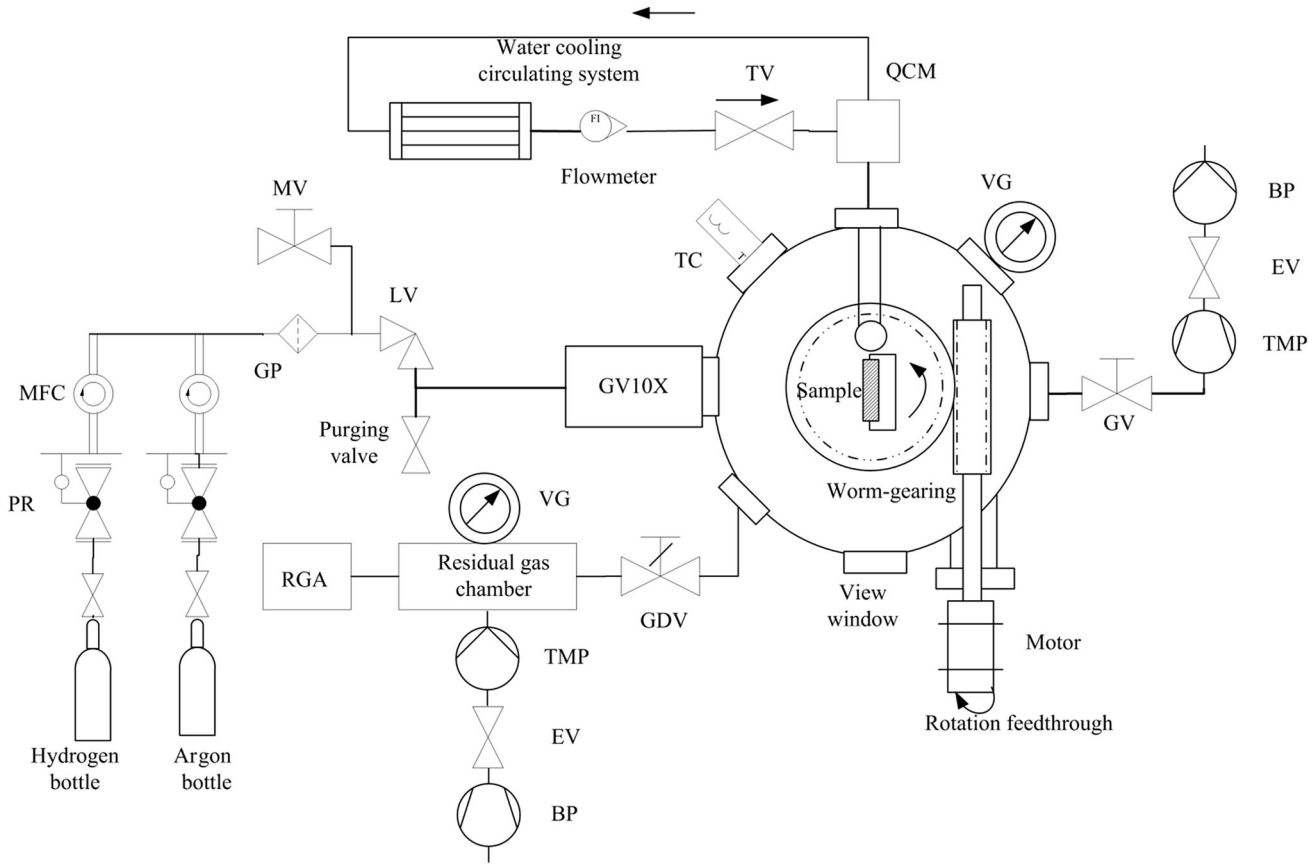

Fig. 2 Conceptual layout of the carbon removal apparatus (*QCM* quartz crystal microbalance, *TV* throttle valve, *VG* vacuum gauge, *TMP* turbomolecular pump, *EV* electro valve, *BP* backing pump, *GV* gating valve, *LV* leaking valve, *TS* temperature sensor, *MV* manual valve, *RGA* residual gas analyzer, *GDV* gas dosing valve, *MFC* mass flow controller, *GP* gas purifier, *PR* pressure reducer)

time of the three steps have been adjusted to zero in Fig. 4. It can be seen from Fig. 4 that the removal rates of the pure H_2 plasma, pure Ar plasma, and Ar/H_2 plasma were 0.048 nm/min, 0.09 nm/min, and 0.408 nm/min, respectively. The removal rate with the combined Ar/H_2 plasma is approximately four times larger than the sum of the separate plasmas at a power of 90 W with the GV10X RF gun and a total pressure of 0.001 mbar. The carbon thickness removed versus time curve clearly demonstrates the synergistic effect of the Ar/H_2 plasma. Compared with the removal of carbon using pure H_2 or Ar plasma, the efficiency was improved by the addition of argon to the hydrogen plasma. It is necessary to discuss the removal mechanism of the enhancement using Ar/H_2 plasma. The mechanism for carbon removal includes two aspects: physical sputtering and chemical erosion.

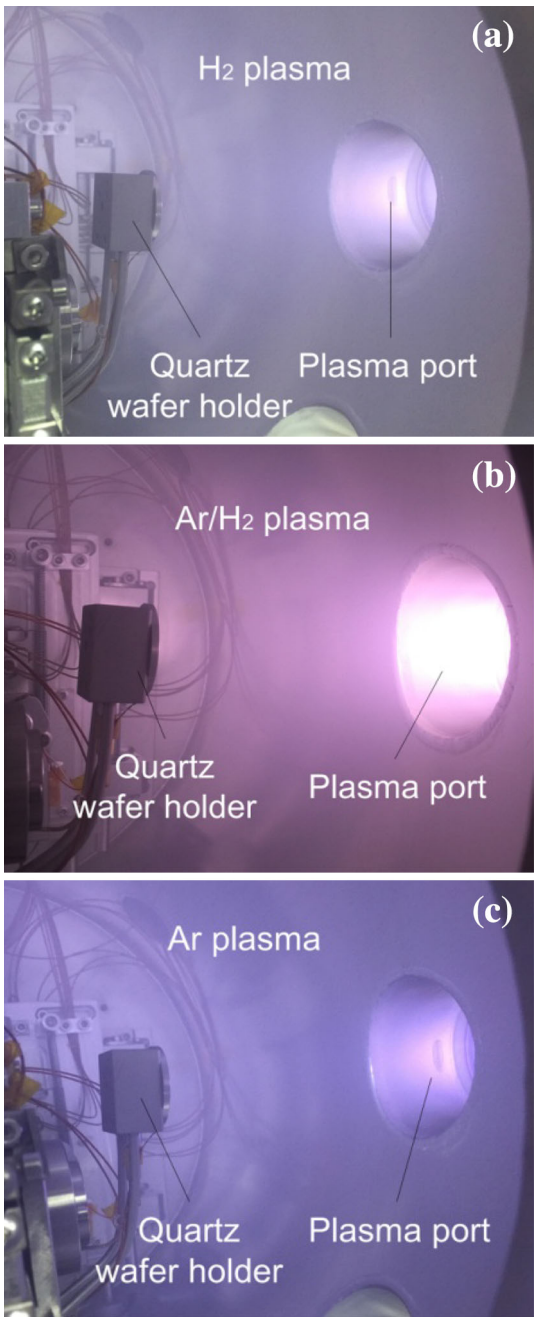

Fig. 3 (Color online) Photographs of RF plasma observed through a quartz window (colored): **a** H_2 plasma, **b** Ar/H_2 plasma, and **c** Ar plasma

3.1.1 *Physical sputtering*

In the mechanisms leading to the erosion of plasma, physical sputtering [17, 18] is capable of removing surface atoms from a solid due to the impact of energetic particles, which results in elastic energy transfer from the incident particles to target atoms. When the energy transferred to surface atoms is below the threshold energy, E_{th}, the sputtering yield is zero. However, when the energy of the incident particles is greater than the threshold energy, surface atoms can be ejected. E_{th} is related to both the surface binding energy of carbon and the mass of the incident particles.

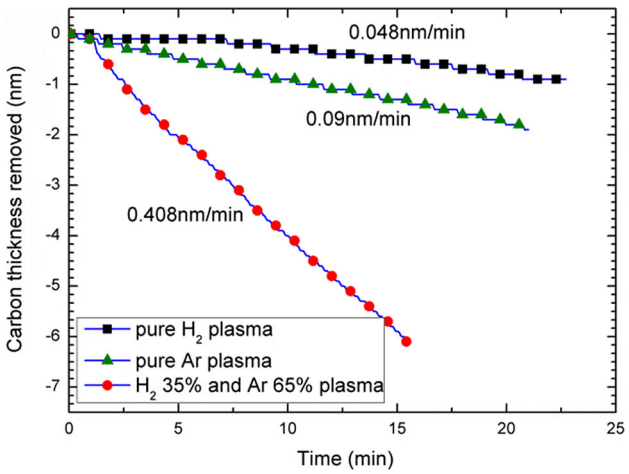

Fig. 4 (Color online) Carbon thickness removed curve versus time

The sputtering mechanism can be described by momentum transport in a collision cascade initiated by the incident particles. This removal mechanism is mainly related to the energy carried by the particles. Physical sputtering is a well-investigated erosion mechanism for the dominant processes. The Bohdansky formula, an empirical equation based on experimental data, is widely used [19]. The sputtering yields of six gases (hydrogen, argon, fluorine, oxygen, nitrogen, and helium) have been calculated using simulation software [20] based on the Bohdansky formula. As shown in Fig. 5, the sputtering yield of the above particles is very low. As with nitrogen, fluoride, and oxygen, the carbon threshold energy is higher than that of

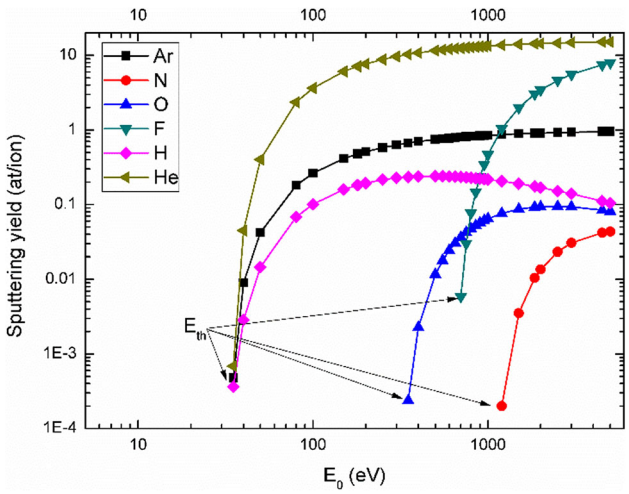

Fig. 5 (Color online) Energy dependence of the sputtering yield and the energy thresholds of different species on carbon by the Bohdansky formula [18]

argon, hydrogen, and helium. Pure Ar plasma is widely used in ion beam etching (IBE) to polish the surface of mirrors [21], but IBE is not suitable for multilayers owing to the potential for serious damage to the upper layers. As for low-pressure plasmas, no accelerating process exits, and thus the energy of the atoms is not very high (less than 300 eV) [22]. However, Ar, as an inert gas, can avoid introducing unnecessary chemical products and facilitate plasma ignition. In other words, the removal rate of the pure Ar plasma in Fig. 4 is mainly attributable to the sputtering effect. In contrast, however, the sputtering effect of the hydrogen plasma and Ar/H_2 plasma on the carbon removal is negligible, and the enhanced removal is caused by the chemical erosion mechanism.

3.1.2 Chemical erosion

Chemical erosion [23] is the formation of volatile molecules on the target surface. The interaction between species in the hydrogen plasma and the deposited carbon can be divided into two steps: hydrogenation and desorption. Generally, the deposited carbon is amorphous, and the orbital hybridization state of the carbon atoms is sp^2. When the hydrogen atoms arrive at the surface, hydrogenation occurs, and the orbital hybridization state of the carbon changes from sp^2 to sp^3 [24]. When hydrogenation is complete, the orbital hybridization state of carbon is transformed to sp^3. When the hydrocarbon molecules accumulate enough energy from collision with the species in the plasma, they will desorb from the surface and escape into the gas. Both hydrogenation and desorption have an effect on the removal rate.

During hydrogenation, radical H atoms first adsorb on the surface and then react with carbon atoms. In a pure hydrogen plasma, the following chemical reaction can occur on the surface:

$$\mathrm{H\,(ads)} + \mathrm{H\,(gas)} \rightarrow \mathrm{H_2\,(gas)}, \quad (1)$$

where (gas) represents atoms or molecules in the gas phase, and (ads) indicates atoms or molecules adsorbed on the surface. In the presence of the above recombination reaction, the reaction efficiency between the adsorbed hydrogen atoms and the deposited carbon is significantly affected.

The composition of the species in the plasma is closely related to the reaction efficiency, and thus, it is necessary to investigate the plasma differences using diagnostic techniques. Mass spectrometry is a common plasma diagnostic technique. RGA was utilized to diagnose the different plasmas by detecting the ion current, which corresponds to the density of species. Different masses represent different types of species in the plasma. The main mass spectra of the different plasmas are shown in Fig. 6. In the pure hydrogen plasma, the primary species is H_3^+, corresponding

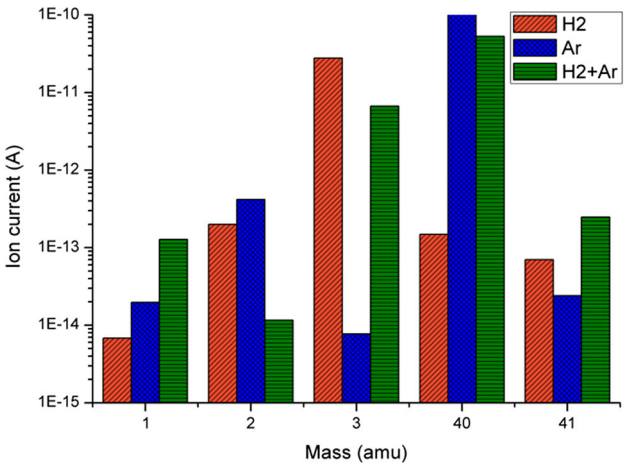

Fig. 6 (Color online) Mass spectra of different plasmas obtained with RGA

to a mass number of 3, which coincides with the results given in Ref. [14]. However, the density of radical H atoms is very small, which is consistent with the efficiency of carbon removal.

Compared to the pure hydrogen plasma, the density of radical H atoms is increased by about one order of magnitude in the Ar/H_2 plasma, as shown in Fig. 6. Annemie et al. [26, 27] suggested that the production of radical H is enhanced in the Ar/H_2 plasma according to reactions (2)–(5), but particularly through reaction (2) by the metastable Ar atom (Ar_m^*) due to the Penning effect.

Quench and dissociation of H_2:

$$\mathrm{Ar_m^* + H_2 \rightarrow 2H + Ar}. \quad (2)$$

Charge transfer:

$$\mathrm{Ar + H^+ \rightarrow Ar^+ + H}. \quad (3)$$

Recombination:

$$\mathrm{e^- + ArH^+ \rightarrow Ar + H} \quad (4)$$

$$\mathrm{H_2^+ + e^- \rightarrow H + H}. \quad (5)$$

As shown in Fig. 6, compared to pure H_2 or Ar plasma, the density of the polyatomic ArH^+ ion corresponding to a mass of 41 is increased significantly in the Ar/H_2 plasma. The formation of ArH^+ can occur in two ways, as given below. Annemie et al. [25] determined that the ArH^+ ions were mainly created through reaction (6).

H-atom transfer:

$$\mathrm{Ar^+ + H_2 \rightarrow ArH^+ + H}. \quad (6)$$

Proton transfer:

$$\mathrm{Ar + H_2^+ \rightarrow ArH^+ + H}. \quad (7)$$

Unlike physical sputtering, the transport of active particles and reaction products is the primary aspect of

chemical erosion. It is believed that the polyatomic ArH^+ ion may transport hydrogen radicals as a gas carrier in the removal of carbon contamination.

In ion-enhanced gas–surface chemistry, Coburn and Winters [23] attributed the mechanism responsible for the Ar^+-enhanced F_2–Si reaction rate to adsorption and desorption. This mechanism has been widely accepted in the field of chemical kinetics and surface processes. It is believed that adsorption and desorption are very important, and in many cases, either of these reactions is the rate-limiting step for a surface process, especially at low energies [24]. The hydrogen–carbon system is very similar to the fluorine–silicon system, and thus, the removal of carbon contamination by an Ar/H_2 plasma can be described by the following sequence: (1) non-dissociative adsorption of gas-phase species on the surface; (2) reaction between the polyatomic ion and deposited carbon atoms and formation of adsorbed product molecules; (3) recombination of the residual ions; and (4) desorption of the product molecules. These steps are illustrated schematically in Fig. 7.

The enhanced removal with Ar/H_2 plasma is related to the steps shown in Fig. 7. Chemical adsorption often occurs on the atomic clean surface, but may not occur on the same surface adsorbed with monolayer gas. The specimen was exposed to the atmosphere before removal was carried out. The gas in the air (mainly nitrogen and oxygen) was thus adsorbed on the surface of the specimen. This adsorption layer cannot be completely removed even under vacuum, but it is removed under the ionic bombardment of the Ar/H_2 plasma, which is helpful for the adsorption of ArH^+ or hydrogen atoms in the plasma.

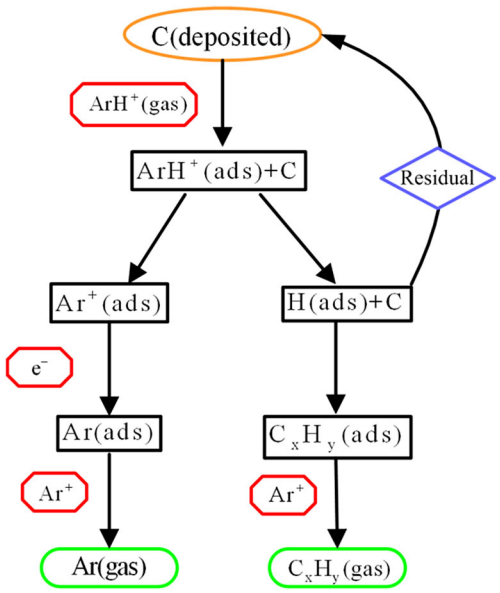

Fig. 7 Flowchart of the reaction between ArH^+ and deposited carbon

As mentioned above, the adsorption layer hinders the reaction of active particles with the deposited carbon. Therefore, the desorption step is important for improving the removal efficiency. The adsorption and desorption of particles on the surface exist in a dynamic equilibrium [28], and the conversion direction of the equilibrium is affected by the vacuum condition, temperature, and other particles. The vacuum situation and temperature of the removal process remain almost unchanged. However, as shown in Fig. 7, argon ions (Ar^+) promote desorption of the products and residual argon atoms. Therefore, for the arrival of active particles on the carbon surface and the removal of volatile products, argon plays a catalytic role in the species transmission.

As mentioned above, there are several approaches by which Ar/H_2 plasma can improve the removal rate of carbon contamination: (1) increasing the concentration of radical hydrogen atoms; (2) expediting the adsorption of hydrogen radicals on the surface of the optics; and (3) increasing the desorption of reaction products.

3.2 Optimized parameters for removal using Ar/H_2 plasma

To remove carbon contamination with a higher efficiency using Ar/H_2 plasma, the optimal parameters should be determined for practical application, including the vacuum pressure, RF output power, and gas mixing ratio.

The carbon removal rates obtained with various process parameters at a feedstock gas mixing ratio of 35% H_2 and 65% Ar are summarized in Table 1. As the experimental data in Table 1 indicate, at different source powers, higher removal rates are obtained at a total pressure of 1×10^{-3} mbar, while the removal rates increase with the power at different pressures. In addition, the highest rate of 0.41 nm/min is obtained at a pressure of 1×10^{-3} mbar and RF power of 90 W. From observation of the experimental results, when the pressure is below 2×10^{-4} mbar, it is difficult to produce plasma because there are fewer molecules in the plasma region to create a cascade that would strike the plasma. The pressure indicates the mean free path of species in plasma. When the pressure is decreased, the mean free path of the radicals increases. Although more radicals are produced at higher pressure, the number of radicals available for removal is increased by lowering the pressure. This is why the GV10X was designed in the "Downstream" style [15, 16].

The gas mixing ratio has a strong effect on the efficiency of the removal rate. With a chamber pressure of 1×10^{-3} mbar, a series of experiments with different source powers and gas mixing ratios was carried out, and the results are shown in Fig. 8.

Table 1 Carbon removal rates at different total pressures and source powers (with a feedstock gas mixing ratio of 35% H_2 and 65% Ar)

Source power (W)	Removal rate (nm/min)				
	2×10^{-4} mbar	5×10^{-4} mbar	1×10^{-3} mbar	5×10^{-3} mbar	1×10^{-2} mbar
30	–	0.13	0.17	0.1	0.13
60	0.26	0.25	0.31	0.24	0.26
90	0.3	0.35	0.41	0.34	0.37

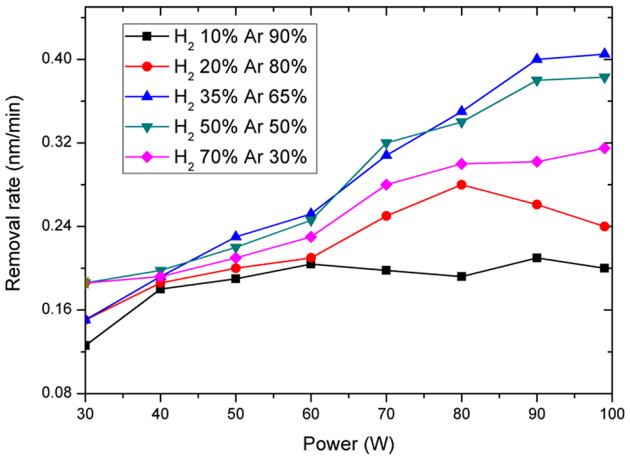

Fig. 8 (Color online) Carbon removal rate curves with varying gas ratio and power

The relationship between the removal rate and the power can be interpreted as the removal rate increasing with increasing power. Higher RF power means that more energy is applied to the particles. With increasing RF power, the energy of the species will increase, which will enhance the desorption of reaction products and result in an improvement in the removal rate.

However, the relationship between the removal rate and the gas mixing ratio was different. When the hydrogen proportion is less than 35%, the removal rate grows continuously with increasing proportion of hydrogen. However, when the proportion of hydrogen exceeded 35%, the reaction rate no longer increased and even decreased. The increase in the proportion of H_2 corresponds to a decrease in the proportion of Ar, and thus, the catalytic effect of Ar on the removal will be weakened. In addition, in the low power range ($\leq$ 60 W), the gas mixing ratio has little effect on the removal rate, while in the high power range ($>$ 60 W), its effect on the removal rate is obvious. It is believed that when the power is higher than 60 W and the proportion of H_2 is greater than 35%, the density of the polyatomic ArH^+ ion will decrease because the energy of the plasma is too high.

3.3 Optimal removal on the multilayer

As in the experimental results mentioned above, the optimal removal parameters are a total pressure of 0.001 mbar, source power of 99 W (the maximum power of the GV10X), and an H_2/Ar mixing ratio of 1:2. A Mo/Si multilayer on a silicon substrate is widely used to improve the reflectivity of X-rays on the beamline [29], as shown in Fig. 9a. For the specimen, a Mo/Si multilayer was coated with amorphous carbon with a thickness of 40 nm, as shown in Fig. 9c. The optimal carbon removal process was performed on the carbon-coated Mo/Si multilayer with half of the specimen shielded, as shown in Fig. 9b. The carbon removal process was performed on two carbon-coated specimens using processing times of 100 min and 60 min. As shown in Fig. 10, the near-normal incident reflectivity of the specimens was detected using an X-ray spectrometer. The results show that compared to the Mo/Si multilayer, the reflectivity of the carbon-coated specimen decreased by about 22.5%. After 100 min of processing, the reflectivity of the specimen is close to that of the pure multilayer films, while the reflectivity of the shielded part is close to that of the carbon-coated multilayer. If the processing time is not adequate, e.g., 60 min, the reflectivity of the specimen exposed to the plasma is only partially recovered. This is consistent with previous experimental results using quartz wafers. Under the optimal removal process, for a carbon layer with a thickness of 40 nm, at least 100 min is required at the removal rate of about 0.4 nm/min.

4 Conclusion

The enhanced removal process of X-ray-induced carbon contamination using RF Ar/H_2 plasma was experimentally investigated in this study. The enhanced carbon removal using Ar/H_2 plasma occurs in the following ways: (1) increasing the concentration of radical hydrogen atoms; (2) expediting the adsorption of hydrogen radicals on the surface of the optics; and (3) increasing the desorption of the reaction products. The optimal removal parameters using Ar/H_2 plasma were determined experimentally. The

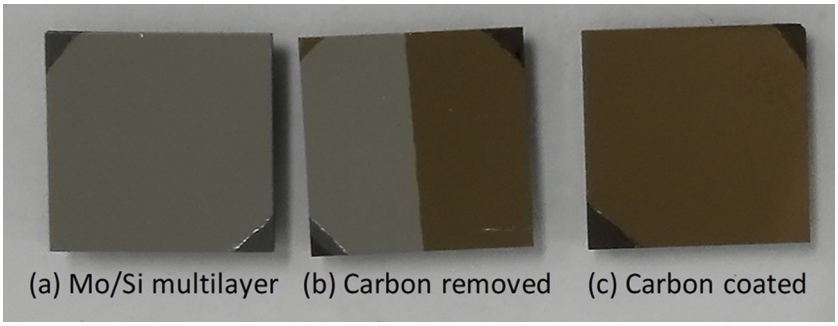

Fig. 9 Carbon-coated Mo/Si multilayer treated with Ar/H_2 plasma

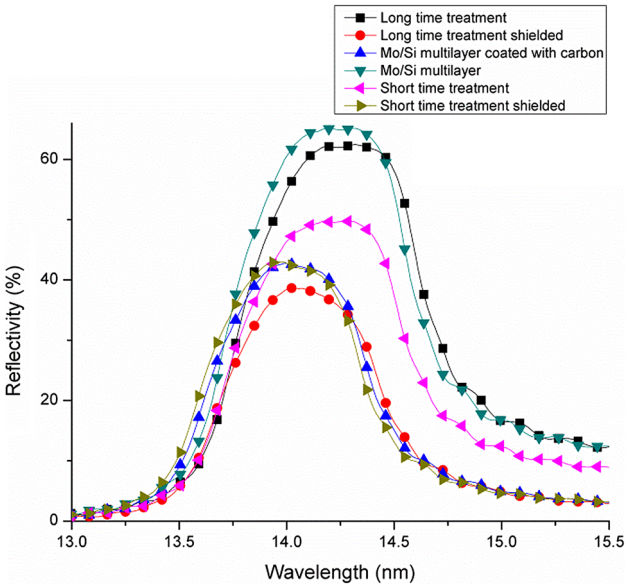

Fig. 10 (Color online) Reflectivity of a carbon-coated Mo/Si multilayer with Ar/H_2 plasma treatment

optimal removal process was performed on a carbon-coated Mo/Si multilayer, and the reflectivity was successfully recovered by removing the carbon contamination. This approach is feasible for use in synchrotron radiation beamlines, X-ray free-electron laser facilities, and even extreme ultraviolet lithography. Further efforts will focus on the realization of in situ carbon removal.

References

1. A. Dolgov, D. Lopaev, C. Lee et al., Characterization of carbon contamination under ion and hot atom bombardment in a tin-plasma extreme ultraviolet light source. Appl. Surf. Sci. **353**, 708–713 (2015). https://doi.org/10.1016/j.apsusc.2015.06.079
2. H. Shin, J. Sporre, R. Raju et al., Reflectivity degradation of grazing-incident EUV mirrors by EUV exposure and carbon contamination. Microelectron. Eng. **86**, 99–105 (2009). https://doi.org/10.1016/j.mee.2008.10.009
3. H. Steffen, K. Manuel et al., Exploring new avenues in high repetition rate table-top coherent extreme ultraviolet sources. Light Sci. Appl. **4**, e320 (2015). https://doi.org/10.1038/lsa.2015.93
4. M. Chen, J. Luo, F. Li et al., Tunable synchrotron-like radiation from centimeter scale plasma channels. Light Sci. Appl. **5**, e16015 (2016). https://doi.org/10.1038/lsa.2016.15
5. M. Xin, K. Safak, Y. Peng et al., Attosecond precision multi-kilometer laser-microwave network. Light Sci. Appl. **6**, e16187 (2017). https://doi.org/10.1038/lsa.2016.187
6. S. Graham, C. Steinhaus, W. Clift, et al., Atomic hydrogen cleaning of EUV multilayer optics, in *Proceedings of SPIE—The International Society for Optical Engineering*, vol. 5037 (2003)
7. J. Chen, E. Louis, R. Harmsen et al., In situ ellipsometry study of atomic hydrogen etching of extreme ultraviolet induced carbon layers. Appl. Surf. Sci. **258**, 7–12 (2011). https://doi.org/10.1016/j.apsusc.2011.07.121
8. E. Pellegrin, I. Šics, J. Reyes-Herrera et al., Characterization, optimization and surface physics aspects of in situ plasma mirror cleaning. J. Synchrotron Radiat. **21**, 300 (2014). https://doi.org/10.1107/S1600577513032402
9. Y. Zhang, H. Luo, Z. Guo et al., Cleaning of carbon-contaminated optics using O_2/Ar plasma. Nucl. Sci. Tech. **28**, 127 (2017). https://doi.org/10.1007/s41365-017-0274-z
10. M. Cuxart, J. Reyes-Herrera, I. Šics et al., Remote plasma cleaning of optical surfaces: cleaning rates of different carbon allotropes as a function of RF powers and distances. Appl. Surf. Sci. **362**, 448 (2016). https://doi.org/10.1016/j.apsusc.2015.11.117
11. T. Akio, K. Takashi, T. Hirokazu et al., In situ removal of carbon contamination from a chromium-coated mirror: ideal optics to suppress higher-order harmonics in the carbon K-edge region. J. Synchrotron Radiat. **22**, 1359–1363 (2015). https://doi.org/10.1107/s1600577515015040
12. S. Pradhan, M. Jeevitha, S. Singh, Plasma cleaning of old Indian coin in H_2–Ar atmosphere. Appl. Surf. Sci. **357**, 445 (2015). https://doi.org/10.1016/j.apsusc.2015.09.026
13. H. Barshilia, A. Ananth, J. Khan et al., Ar + H_2 plasma etching for improved adhesion of PVD coatings on steel substrates. Vacuum **86**, 1165–1173 (2012). https://doi.org/10.1016/j.vacuum.2011.10.028
14. E. Malykhin, D. Lopaev, A. Rakhimov et al., Plasma cleaning of multilayer mirrors in EUV lithography from amorphous carbon contaminations. Mosc. Univ. Phys. Bull. **66**, 184–189 (2011). https://doi.org/10.3103/S0027134911020111
15. G.J. Gorin, US 6263831 B1, 2001
16. G.J. Gorin, US 7015415 B2, 2006
17. C. García-Rosales, Erosion processes in plasma-wall interactions. J. Nucl. Mater. **211**, 202–214 (1994). https://doi.org/10.1016/0022-3115(94)90348-4
18. R. Clark, D. Reiter (eds.), *Nuclear Fusion Research: Understanding Plasma-Surface Interactions* (Springer, Berlin, 2005), pp. 203–206

19. J. Bohdansky, A universal relation for the sputtering yield of monatomic solids at normal ion incidence. Nucl. Instrum. Methods Phys. Res. Sect. B **2.1–3**, 587–591 (1984). https://doi.org/10.1016/0168-583x(84)90271-4
20. W. Eckstein, *Computer Simulation of Ion-Solid Interaction*, Springer Series in Material Science (Springer, Berlin, 1991), p. 207
21. N. Chkhalo, M. Mikhailenko, A. Mil'kov et al., Effect of ion beam etching on the surface roughness of bare and silicon covered beryllium films. Surf. Coat. Technol. **311**, 351–356 (2017). https://doi.org/10.1016/j.surfcoat.2017.01.023
22. D. Sidorov, N. Chkhalo, M. Mikhailenko et al., Sputtering of carbon using hydrogen ion beams with energies of 60–800 eV. Nucl. Instrum. Methods B **387**, 73–76 (2016). https://doi.org/10.1016/j.nimb.2016.10.007
23. J. Coburn, H. Winters, Ion- and electron-assisted gas-surface chemistry—an important effect in plasma etching. J. Appl. Phys. **50**, 3189 (1979). https://doi.org/10.1063/1.326355
24. M. Lieberman, A. Lichtenberg, *Principles of Plasma Discharges and Materials Processing*, 2nd edn. (Wiley, Hoboken, 2005), pp. 303–304
25. M. Wittmann, J. Küppers, A model of hydrogen impact induced chemical erosion of carbon based on elementary reaction steps. J. Nucl. Mater. **227**, 186–194 (1996). https://doi.org/10.1016/0022-3115(95)00150-6
26. A. Bogaerts, R. Gijbels, Hybrid Monte Carlo-fluid modeling network for an argon/hydrogen direct current glow discharge. Spectrochim. Acta Part B **57**, 1071–1099 (2002). https://doi.org/10.1016/S0584-8547(02)00047-2
27. A. Bogaerts, R. Gijbels, Effects of adding hydrogen to an argon glow discharge: overview of relevant processes and some qualitative explanations. J. Anal. At. Spectrom. **15**, 441–449 (2000). https://doi.org/10.1039/A909779A
28. Q. Zheng, X. Wang, S. Gao, Adsorption equilibrium of hydrogen on graphene sheets and activated carbon. Cryogenics **61**, 143–148 (2014). https://doi.org/10.1016/j.cryogenics.2014.01.005
29. S. Bajt, M. Prasciolu, H. Fleckenstein et al., X-ray focusing with efficient high-NA multilayer Laue lenses. Light Sci. Appl. **7**, 17162 (2018). https://doi.org/10.1038/lsa.2017.162